ARTICLE

Viral infection modulates Qa-1^b in infected and bystander cells to properly direct NK cell killing

Maria Ferez[1], Cory J. Knudson[1], Avital Lev[2], Eric B. Wong[1], Pedro Alves-Peixoto[1,3,4], Lingjuan Tang[1], Colby Stotesbury[1], and Luis J. Sigal[1]

Natural killer (NK) cell activation depends on the signaling balance of activating and inhibitory receptors. CD94 forms inhibitory receptors with NKG2A and activating receptors with NKG2E or NKG2C. We previously demonstrated that CD94-NKG2 on NK cells and its ligand Qa-1^b are important for the resistance of C57BL/6 mice to lethal ectromelia virus (ECTV) infection. We now show that NKG2C or NKG2E deficiency does not increase susceptibility to lethal ECTV infection, but overexpression of Qa-1^b in infected cells does. We also demonstrate that Qa-1^b is down-regulated in infected and up-regulated in bystander inflammatory monocytes and B cells. Moreover, NK cells activated by ECTV infection kill Qa-1^b–deficient cells in vitro and in vivo. Thus, during viral infection, recognition of Qa-1^b by activating CD94/NKG2 receptors is not critical. Instead, the levels of Qa-1^b expression are down-regulated in infected cells but increased in some bystander immune cells to respectively promote or inhibit their killing by activated NK cells.

Introduction

Natural killer (NK) cells are innate lymphocytes that become activated early during viral infections and can protect from viral disease by containing virus replication and spread before the adaptive immune response develops (Diefenbach and Raulet, 2001). Similar to adaptive CTLs, a major mechanism of NK cell's antiviral protection is the killing of infected cells. This process requires direct interaction of the CTL or NK cell with the target cell and most commonly involves the exocytosis of cytolytic granules carrying the membrane pore-forming protein perforin and pro-apoptotic enzymes such as granzyme B, which enters the target cell cytosol (Fehniger et al., 2007; Sun and Lanier, 2011). To avoid immunopathology due to indiscriminate killing of uninfected cells, the activation and ability of CTL and NK cells to distinguish between infected and uninfected cells must be tightly controlled. In CTL, this is mainly achieved through the specific recognition of viral peptides bound to MHC molecules by means of the antigen-specific TCR. Because NK cells lack an antigen-specific receptor, they instead rely on the signaling balance of relatively large numbers of inhibitory and activating receptors that respectively prevent or promote the

killing of target cells (Diefenbach and Raulet, 2001; Lanier, 1998; Sun and Lanier, 2011). To mount a protective NK cell response, the activating receptor signals need to overcome the inhibitory signals. The expression of specific inhibitory and activating receptors varies between the NK cells of an individual, creating an NK cell repertoire. An important group of NK cell receptors are encoded within a locus called the NK complex (NKC), which is located in chromosome 12 in humans and 6 in mice. These receptors are specific for MHC class I (MHC-I) or MHC-I–like molecules, including the human killer-cell Ig-like receptors, the rodent Ly49 receptors, and the human or rodent C-type lectins NKG2D and CD94-NKG2 (A, C, E; Long, 1999; Yokoyama and Seaman, 1993).

CD94, NKG2A, NKG2C, and NKG2E are conserved between humans and mice and are respectively encoded by *Klrd1*, *Klrc1*, *Klrc2*, and *Klrc3*. CD94 alternatively forms a heterodimeric inhibitory receptor with NKG2A or activating receptors with NKG2C and NKG2E (Lanier, 1998). CD94-NKG2 heterodimers are generally believed to be expressed in ~50% of NK cells, with the vast majority of them being CD94-NKG2A, at least under

steady-state conditions (Vance et al., 1999; Vance et al., 1998; Vance et al., 1997). CD94-NKG2 heterodimers are also expressed in activated T cells (Rapaport et al., 2015).

The ligands for CD94-NKG2 heterodimers are the nonclassical MHC-I molecule Qa-1[b] in mice (Vance et al., 1998; Zeng et al., 2012) and HLA-E in humans (Braud et al., 1998; Lee et al., 1998; Sullivan et al., 2007). Upon binding Qa-1[b], CD94-NKG2A transmits intracellular inhibitory signals by recruiting the protein tyrosine phosphatases SHP1 and SHP2 (Kabat et al., 2002; Le Dréan et al., 1998). On the other hand, the activating receptors (CD94-NKG2C/E) transmit activating signals through the transmembrane adaptor DAP10 or DAP12. In humans, NKG2C and NKG2E directly bind DAP10/12 (Call et al., 2010), while CD94 is the molecule responsible for binding DAP10/12 in mice (Saether et al., 2011).

Mousepox is a deadly murine disease caused by ectromelia virus (ECTV), an orthopoxvirus homologue to the human pathogen variola virus, the causative agent of smallpox. ECTV infects all mice, but the outcome of infection differs depending on the mouse strain. While some strains such as BALB/c, DBA/2, and A/J are susceptible, developing classic pox lesions on the skin and succumbing to the infection within the first 7–14 d postinfection (dpi), other strains such as C57BL/6 (B6) and 129 resist the infection without overt signs of disease (Wallace and Buller, 1985). While multiple immune mechanisms are implicated in this resistance (Sigal, 2016), early studies showed that a gene called Resistance to Mousepox 1 (Rmp1) mapped to the NKC, suggesting a role for NK cells in ECTV control (Brownstein et al., 1991). Later work demonstrated that depletion of NK cells or NK cell deficiencies, such as in aged mice, result in susceptibility to lethal mousepox, highlighting the important role of NK cells in the control of ECTV (Delano and Brownstein, 1995; Fang et al., 2008; Fang et al., 2010; Jacoby et al., 1989; Parker et al., 2007).

In previous work, we demonstrated that CD94 deficiency renders B6 mice highly susceptible to lethal mousepox. The inability of CD94-deficient (Klrd1^{−/−}) mice to control ECTV was due to impaired NK cell function because its effects on virus control occurred early, before the T cell response developed. Also, CD8 T cells from CD94-deficient mice mounted normal responses when transferred into WT mice (Fang et al., 2011). Reporter assays provided indirect evidence that activating CD94-NKG2E synergized with NKG2D (an activating receptor that does not pair with CD94) to achieve optimal NK cell activation during ECTV infection (Fang et al., 2011). However, testing this hypothesis directly was not possible because there were no detection antibodies or genetically modified mice lacking activating NKG2E or NKG2C. Later work in the Colonna laboratory demonstrated that male, but not female, mice deficient in NKG2A (klrd1^{−/−}) succumbed to mousepox. Their work also suggested impaired CD8 T cell control due to antigen-induced cell death in the absence of CD94-NKG2A inhibitory signals (Rapaport et al., 2015). Yet, based on results suggesting that activating NKG2s were not expressed by NK cells, these authors did not analyze possible NK cell dysfunctions.

Herein, we continued to study how CD94-NKG2s contribute to NK cell protection from mousepox. First, we generated NKG2E (Klrc3^{−/−})– and NKG2C (Klrc2^{−/−})–deficient mice in a B6
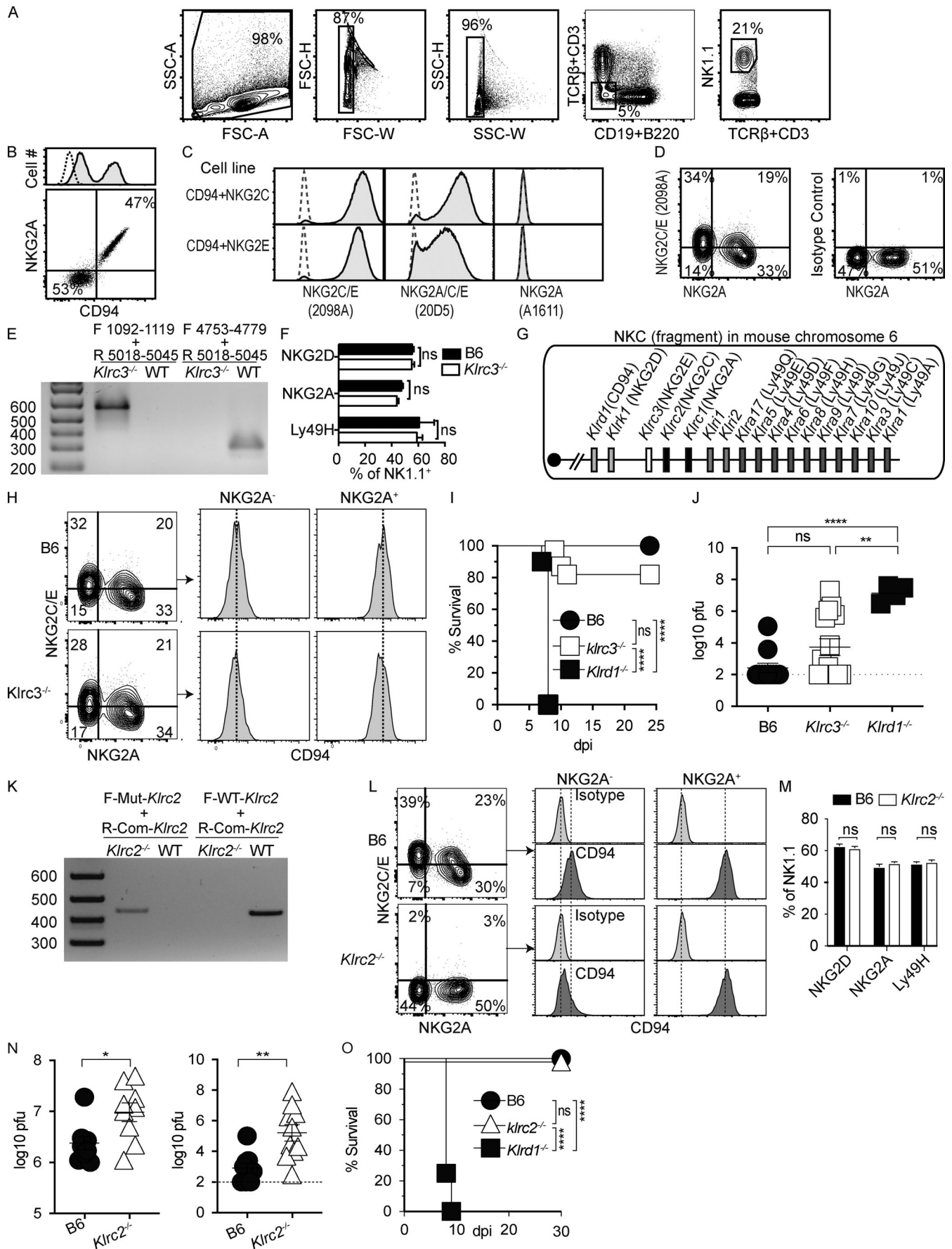
background. We found that they mostly survived ECTV challenge without signs of disease, despite the fact that activating NKG2C is commonly expressed by ∼50% of NK cells. Therefore, in contrast to CD94, activating CD94-NKG2 receptors are not essential to survive mousepox. We also found that recombinant ECTV expressing Qa-1[b] is more pathogenic than WT ECTV in B6 mice, indicating that Qa-1[b] in infected cells is detrimental for virus control. Moreover, we found that infection of mice with WT ECTV causes Qa-1[b] down-regulation in infected and up-regulation in uninfected bystander monocytes (MOs) and B cells. Finally, we discovered that Qa-1[b] expression protects noninfected cells in vitro and in vivo from killing by NK cells activated by ECTV infection. Together, these results indicate that CD94, possibly paired to NKG2A, may restrain NK cell–mediated killing of uninfected bystander cells and that Qa-1[b] down-regulation in infected cells identifies them as killing targets. Thus, Qa-1[b] is a switch that allows activated NK cells to distinguish friend from foe, likely using CD94-NKG2A inhibitory receptors.

Results

Mice deficient in NKG2E or NKG2C are resistant to lethal mousepox

It is commonly thought that CD94/NKG2s are expressed in ∼50% of NK cells and the majority correspond to CD94/NKG2A. This view results from the finding that NKG2A mRNA represents 95% of the total NKG2 mRNA in NK cells (Vance et al., 1999) as well as from costaining of NK cells with mAbs A16ll to B6 NKG2A and 20d5 to all NKG2s (Vance et al., 2002). Also, based on costaining of NK cells from B6 and NKG2A-deficient mice (Klrc1^{−/−}) with anti-NKG2s and anti-CD94 (18d3), it was concluded that NKG2C and NKG2E are not expressed in NK cells (Rapaport et al., 2015). Plotting NK1.1^{+} cells (Fig. 1 A) for expression of NKG2A (16a11) and CD94 (18d3) shows high correlation in the upper right gate (Fig. 1 B, dot plot). Yet, when comparing the staining of CD94 with its isotype control, it becomes apparent that most NKG2A^{−} cells, traditionally also considered CD94^{−}, express CD94 but at low levels (CD94^{low}; Fig. 1 B, top histogram), a fact that has been noted before (Rapaport et al., 2015). Rabbit IgG mAb (2098A) anti-NKG2C is nonreactive with NKG2A. Accordingly, Ba/F3 cells transfected with CD94 and NKG2C stained with 2098A (unlabeled 2098A followed by donkey anti-rabbit polyclonal IgG labeled with Alexa 647). As expected, they also stained with anti–NKG2A/C/E (20D5) but not with anti-NKG2A (16a11). Yet, 2098A also stained Ba/F3 cells transfected with CD94 and NKG2E, indicating it is anti–NKG2C/E (Fig. 1 C). When we analyzed the NK cells in the spleen of B6 mice, we found that the vast majority (if not all) of the NKG2A^{−} NK cells were NKG2C/E[+] and that ∼1/3 of the NKG2A^{+} NK cells were also NKG2C/E[+] (Fig. 1 D). Thus, contrary to the prevalent view (Rapaport et al., 2015; Vance et al., 2002; Vance et al., 1999), activating CD94/NKG2s are expressed in ∼50% of NK cells under basal conditions.

As mentioned above, previous results led us to hypothesize that activating CD94-NKG2E on NK cells was important for resistance to ECTV (Fang et al., 2011). To test this directly, we used

Ferez et al.
Qa-1[b] in viral infection

Journal of Experimental Medicine   2 of 13
https://doi.org/10.1084/jem.20201782

Figure 1.   **Mice deficient in NKG2E or NKG2C are resistant to mousepox. (A)** Representative gating strategy to identify NK cells. **(B)** Representative contour plot gated on NK cells showing the expression of CD94 and NKG2A (bottom) and histogram for CD94 (filled, black line) and corresponding isotype control (dashed line; top). **(C)** Representative histograms from two experiments showing staining of the indicated cell lines with the indicated antibodies (filled histograms, black lines) or isotype control (dashed lines). **(D)** Representative contour plots gated on NK cells showing staining for NKG2A and NKG2C/E as determined with mAb 2098A (left) or isotype control (right). **(E)** Example of PCR genotyping of $Klrc3^{-/-}$ and WT B6 using the indicated primers. **(F)** Graph showing the frequency of NK cells expressing the indicated receptors in spleens from naive B6 and $Klrc3^{-/-}$ mice. Data are representative of two similar experiments with three mice/group. Data were analyzed using the t test. **(G)** Representation of the portion of the NKC complex where NKG2 and CD94 genes are located in mouse chromosome 6. **(H)** Representative contour plots (left) showing the expression of NKG2A and NKG2C/E in NK cells from B6 and $Klrc3^{-/-}$ mice and histograms showing the expression of CD94 in gated NKG2A⁻ and NKG2A⁺ NK cells (right) from the same mice. The dashed vertical lines intersect the MFIs and are placed to facilitate the visual comparison of the histograms. **(I)** The indicated mice were infected with 3,000 pfu ECTV in the footpad, and survival was monitored. Data are displayed as a combination of three independent experiments with a total of 10–31 mice/group. Data were analyzed using the log-rank test. **(J)** The indicated mice were infected with ECTV, and at 7 dpi the virus loads in spleens of individual mice were determined by plaque assay. The dotted line indicates limit of detection. Data correspond to three individual experiments combined with a total of 4–13 mice/group. Data were analyzed using ANOVA with correction for multiple comparisons. **(K)** Example of PCR genotyping of $Klrc2^{-/-}$ and WT B6 mice using the indicated primers. **(L)** Contour plots (left) showing the expression of NKG2A and NKG2C/E in NK cells from B6 and $Klrc2^{-/-}$ mice and histograms (right) showing the expression of CD94 or isotype control in gated NKG2A⁻ and NKG2A⁺ NK cells from the same mice. Dashed vertical lines intersect MFIs and are placed to facilitate the visual comparison of histograms. Data correspond to a representative mouse from two experiments with three or four mice/group. **(M)** Graph showing the frequency of NK cells expressing the indicated receptors in spleens from naive B6 and $Klrc2^{-/-}$ mice. Data are representative of two similar experiments with four mice/group. Data were analyzed using the t test. **(N)** The indicated mice were infected with ECTV, and at 5 (left) or 7 (right) dpi, the virus loads, indicated as pfu, in spleens of individual mice were determined by plaque assay. The dotted line indicates limit of detection. Data correspond to two individual experiments combined with a total of 8–13 mice/group. Data were analyzed using the t test. **(O)** The indicated mice were infected with 3,000 pfu ECTV in the footpad, and survival was monitored. Data are displayed as a combination of two independent experiments with a total of 9 or 10 mice/group. Data were analyzed using the log-rank test. For all statistics in the figure, *, $P \leq 0.05$; **, $P \leq 0.001$; ****, $P \leq 0.0001$. All error bars indicate mean ± SEM.

traditional embryo stem (ES) cell blastocyst microinjection technology to make NKG2E-deficient mice ($Klrc3^{-/-}$), where positions 1214–4792 (3,578 bp) of the 7,249-bp $Klrc3$ gene (NCBI Reference Sequence NC_000072.7, *Mus musculus* strain C57BL/6J chromosome 6, GRCm39, accession no. NC_000072 REGION: complement [129613226..129620474]) comprising exons 3–5 and part of their flanking sequences was replaced by an irrelevant 218-bp fragment containing residual flippase recognition target (FRT) and LoxP1 sequences (Fig. S1 A). PCR analysis of tail DNA with forward primer positions 1092-1119 (F 1092-1119) and reverse primer positions 5018-5045 (R 5018-5045), which flank the deleted 1214–4792 area of the WT allele, demonstrated an expected mutant amplicon of 592 bp in $Klrc3^{-/-}$ but not in WT B6 mice (a possible 3,953-bp WT amplicon was not resolved by the PCR conditions used). Conversely, PCR using forward primer positions 4753-4779 (F 4753-4799), which is within the deleted 1214–4792 area in $Klrc3^{-/-}$ mice, and R 5018-5045 showed an expected 293-bp WT amplicon in WT but not in $Klrc3^{-/-}$ mice (Fig. 1 E and Fig. S1 A). Sanger sequencing of the 592-mutant band demonstrated the expected sequence composition comprising 5′ and 3′ flanking areas of exons 3 and 5, respectively, and the 218-bp insert with the FRT and LoxP sequences (Fig. S1 B). Analysis of $Klrc3^{-/-}$ mice splenocytes showed normal frequencies of NKG2D⁺, NKG2A⁺, and Ly49H⁺ NK cells (Fig. 1 F), which are encoded in the NKC and closely linked to $Klrc3$ (Fig. 1 G). They also stained with anti-CD94 and anti–NKG2C/E similarly to B6 mice (Fig. 1 H), suggesting that NKG2C but not NKG2E is normally expressed in NK cells. Staining for additional NK cell receptors and maturation markers suggested normal NK cell development and phenotype (Fig. S1 C), which was consistent with the normal NK cell development previously observed in CD94-deficient ($Klrd1^{-/-}$) mice (Orr et al., 2010). When challenged with ECTV, a small percentage of $Klrc3^{-/-}$ mice succumbed by 10–11 dpi and all B6 mice survived, but the difference was not statistically significant. In comparison, all $klrd1^{-/-}$ mice

died from mousepox before 9 dpi, and the difference with $Klrc3^{-/-}$ and B6 mice was highly significant (Fig. 1 I). Also, while a fraction of $Klrc3^{-/-}$ mice had higher virus titers in their spleens, the overall titers did not differ significantly with those of B6 mice and were significantly lower than in $klrd1^{-/-}$ mice (Fig. 1 J). Thus, in contrast to CD94, NKG2E is not essential for resistance to lethal mousepox.

Given the negative result with NKG2E, we decided to test whether NKG2C was important for resistance to mousepox. With this purpose, we targeted the $Klrc2$ gene using the improved genome editing via oviductal nucleic acids delivery (i-GONAD) method of CRISPR/Cas9 gene editing (Gurumurthy et al., 2019; Ohtsuka et al., 2018). A founder mouse had a GA insertion after position 438 of transcript NCBI Reference Sequence NM_010653.4. This resulted in an early termination codon 40 bp downstream of the insertion (Fig. S1 D). The progeny of this mouse was bred to homozygosity to obtain Klrc2-deficient ($Klrc2^{-/-}$) mice. PCR analysis of tail DNA showed that amplification with a forward primer specific for mutant $Klrc2$ (F-Mut-$Klrc2$) containing the GA insertion and a common reverse primer specific for both WT and mutant $Klrc2$ (R-Com-$Klrc2$) amplified a 438-bp band in $Klrc2^{-/-}$ but not in WT mice, while amplification with a forward primer specific for WT $Klrc2$ (F-WT-$Klrc2$) and R-Com-$Klrc2$ amplified a band of 439 bp in WT but not in $Klrc2^{-/-}$ mice (Fig. 1 K). NK cells in $Klrc2^{-/-}$ mice stained normally with anti-NKG2A but did not stain with anti–NKG2C/E (Fig. 1 L, left contour plots), confirming that NKG2C is normally expressed in the NK cells of B6 mice. Also, while the frequency and mean fluorescence intensity (MFI) of CD94^high NK cells in $Klrc2^{-/-}$ mice was normal, the fluorescence intensity of the CD94^low peak was reduced to levels similar to isotype control (Fig. 1 L, right histograms). This suggested that they did not express CD94 due to the absence of a pairing partner. Together with the data from $Klrc3^{-/-}$ mice, these data suggest that CD94-NKG2C but not CD94-NKG2E is normally present at the

surface of ~50% of NK cells in WT mice and that all activating CD94-NKG2s are absent in $Klrc2^{-/-}$ but not in $Klrc3^{-/-}$ mice. Also, $Klrc2^{-/-}$ mice had normal frequencies of $NKG2D^+$, $NKG2A^+$, and $Ly49H^+$ NK cells (Fig. 1 M) and other NK cell receptors and maturation markers (Fig. S1 C), indicating that the mutation did not affect the expression of neighboring genes or NK cell development. When challenged with ECTV, $Klrc2^{-/-}$ mice had significantly increased but highly variable virus loads at 5 and 7 dpi in their spleens compared with WT B6 mice (Fig. 1 N) but were nonetheless fully resistant to lethal mousepox (Fig. 1 O). The data with $Klrc2^{-/-}$ and $Klrc3^{-/-}$ mice indicate that while deficiency in activating CD94-NKG2 heterodimers may partially affect virus control, it is not the main reason why CD94-deficient mice are highly susceptible to lethal mousepox.

Qa-1[b] interaction with CD94-NKG2 on NK cells is required for resistance to mousepox

We previously showed that compared with B6, mice deficient in Qa-1[b] ($H2$-$T23^{-/-}$), the ligand for all CD94-NKG2 heterodimers, had faster ECTV dissemination and were highly susceptible to lethal mousepox (Fang et al., 2011). Thus, we investigated the role of CD94-NKG2 interaction with Qa-1[b] in more detail. First, we looked at the effect of ECTV on overall Qa-1[b] expression in vivo. Compared with naive, Qa-1[b] was up-regulated in splenocytes at 5 dpi, which is the peak of the NK response to ECTV (Fig. 2 A; Fang et al., 2008). When analyzed by cell type, B cells expressed significantly more Qa-1[b] than other immune cells in naive mice. At 5 dpi, B cells and MOs strongly up-regulated Qa-1[b] while T cells and NK cells did minimally so (Fig. 2 B). Of note, MOs and B cells, but not T cells or NK cells, are main targets of ECTV infection. Also, inflammatory MOs (iMOs) have critical roles in the protective innate immune response to ECTV in the draining lymph node (dLN; Wong et al., 2018; Xu et al., 2015).

Next, we used the Qa-1[b] knock-in mouse strain $H2$-$T23^{R72A}$, which has a mutation in $H2$-$T23$ resulting in an R→A substitution in position 72 of Qa-1[b]. This substitution prevents the interaction of Qa-1[b] with CD94-NKG2 but does not interfere with its interaction with the TCR (Lu et al., 2007). Qa-1[b] was present and up-regulated to similar levels in B cells and MOs of WT and $H2$-$T23^{R72A}$ mice but was absent in control $H2$-$T23^{-/-}$ mice (Fig. 2 C). Flow cytometry of splenic NK cells from $H2$-$T23^{R72A}$ stained with Abs to various NK cell receptors and maturation markers, indicating overall normal NK cells in these mice (Fig. S1 C).

Having found normal expression and up-regulation of Qa-1[b] and normal NK cell development in $H2$-$T23^{R72A}$ mice, we determined their resistance to mousepox using B6 and $H2$-$T23^{-/-}$ mice as controls. As previously shown (Fang et al., 2011), $H2$-$T23^{-/-}$ mice were significantly more susceptible to lethal mousepox than B6 mice, with almost 60% succumbing to the infection. Notably, $H2$-$T23^{R72A}$ mice were even more susceptible, with 100% dying before 11 dpi (Fig. 2 D). Consistent with this finding, $H2$-$T23^{R72A}$ mice had higher virus loads than WT mice in their spleens and livers at 3 and 7 dpi (Fig. 2 E). Because NK cells and not T cells control the spread of ECTV from the dLN to the spleen at 3 dpi (Fang et al., 2008; Fang et al., 2011), these data indicate that the direct interaction of Qa-1[b] with CD94-NKG2 on NK cells is required for optimal control of ECTV spread and resistance to mousepox.

Ectopic overexpression of Qa-1[b] in infected cells increases susceptibility to mousepox

The data with $Klrc2^{-/-}$ and $Klrc3^{-/-}$ mice suggested that activating signals to NK cells through CD94–NKG2C/E are not necessary for mousepox resistance. Yet, our results above suggested that up-regulation of Qa-1[b] in MOs and B cells and its interaction with CD94-NKG2 on NK cells could be required for optimal resistance to mousepox. Thus, we hypothesized that ectopic expression of Qa-1[b] by ECTV would result in its attenuation in $H2$-$T23^{R72A}$ mice. To test this, we engineered ECTV virus expressing Qa-1[b] together with the red fluorescent protein dsRed (ECTV–Qa-1[b]–dsRed) using methodologies previously described (Roscoe et al., 2012). ECTV–Qa-1[b]–dsRed replicated to similar levels as WT ECTV in one-step (Fig. 3 A) and multistep (Fig. 3 B) growth assays, indicating that ECTV–Qa-1[b]–dsRed did not have a major direct effect on virus replication in tissue culture. Next, we made bone marrow–derived macrophages (BMDMs) by culturing bone marrow cells for 7 d in the presence of L cell supernatant. Overnight infection of BMDMs with 5 plaque-forming units (pfu) of ECTV–Qa-1[b]–dsRed resulted in increased Qa-1[b] expression compared with uninfected BMDMs. Conversely, infection of BMDMs with 5 pfu WT ECTV resulted in decreased Qa-1[b] expression (Fig. 3 C), suggesting that infection decreases, rather than increases, endogenous Qa-1[b] expression in infected cells. At 3 dpi, dsRed+ cells in the dLNs of ECTV–Qa-1[b]–dsRed-infected mice had higher fluorescence intensity for Qa-1[b] than in mice infected with control ECTV-dsRed (Fig. 3 D). As expected, B6 mice survived and $H2$-$T23^{R72A}$ succumbed to control ECTV-dsRed infection. However, contrary to our expectation, not only $H2$-$T23^{R72A}$ but also WT B6 mice succumbed to ECTV–Qa-1[b]–dsRed challenge (Fig. 3 E), with increased virus titers in their spleens at 7 dpi (Fig. 3 F). These data indicate that Qa-1[b] up-regulation in infected cells favors rather than curtails viral replication and disease. This strongly suggested that by imparting inhibitory signals to NK cells, Qa-1[b] protects infected cells from NK cell cytolytic killing, thereby promoting virus replication.

ECTV induces Qa-1[b] down-regulation in infected cells and up-regulation in bystander cells in vivo

The data above showed that expression of Qa-1[b] is increased in splenocytes during ECTV infection and that Qa-1[b] on infected cells is detrimental for mousepox survival. This seemed to contradict the finding that Qa-1[b] interaction with NK cells is required for resistance to mousepox. A possible clue to the problem emerged from Fig. 3 C, showing that BMDMs infected with WT ECTV down-regulated Qa-1[b]. Thus, we used ECTV-dsRed to determine whether the up-regulation of Qa-1[b] occurred in infected or uninfected iMOs and B cells in the dLN. We found that compared with the nondraining LN, the increase in Qa-1[b] expression in the dLNs at 3 dpi occurred in uninfected (dsRed−) B cells and iMOs, and similar to BMDMs, it was significantly decreased in infected (dsRed+) iMOs (Fig. 4; this is not possible to do in spleen because we cannot identify infected cells by flow cytometry, likely because they are present in too small frequency in this organ). These results suggested that rather than promoting NK cell killing of infected cells through
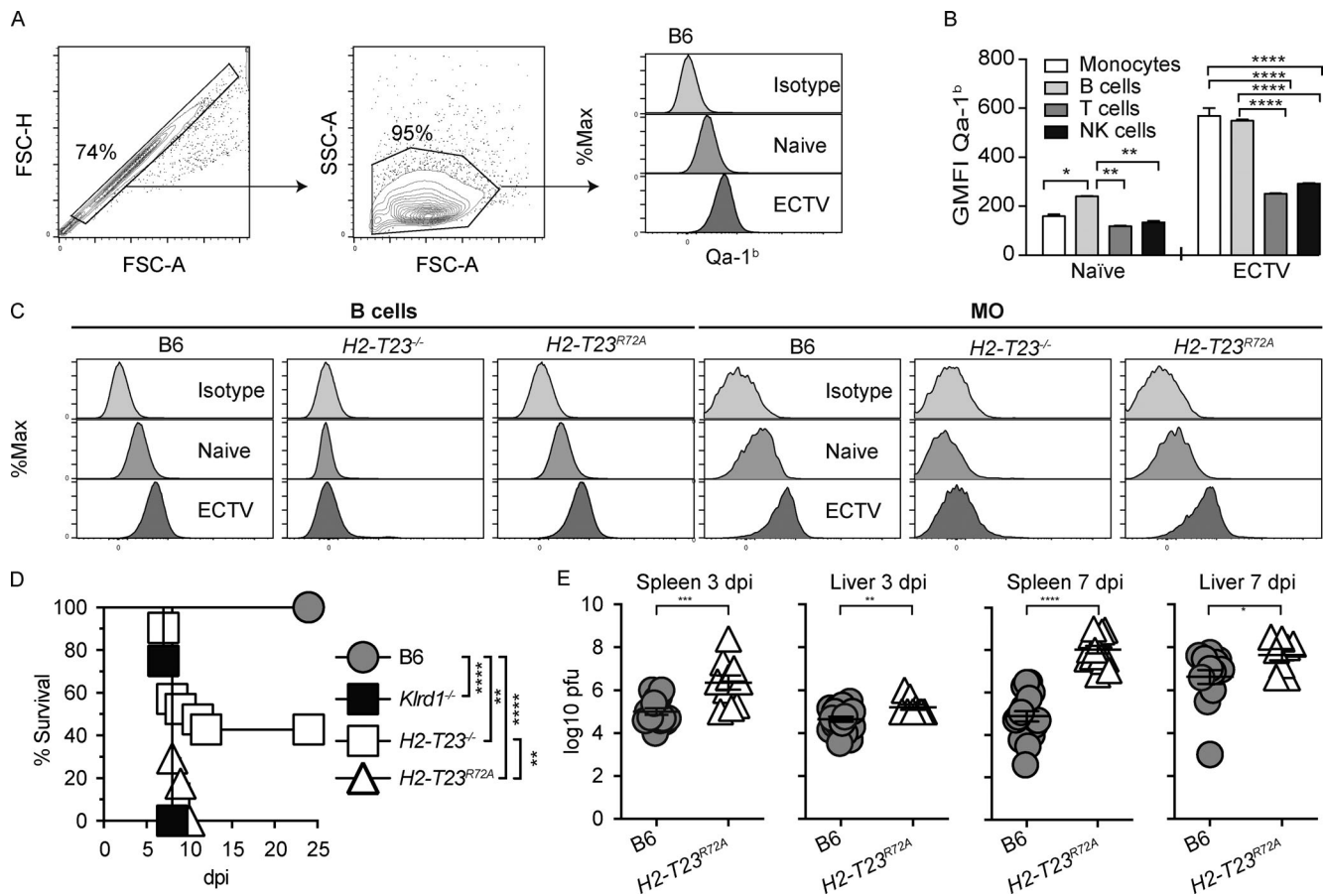
Figure 2. Qa-1^b interaction with CD94-NKG2 on NK cells is required for optimal resistance to mousepox. (A) Flow cytometry analysis of Qa-1^b expression in splenocytes from B6 mice that were naive or at 5 dpi with ECTV. Expression of Qa-1^b is shown in the histogram plot. Staining with an isotype control is shown for comparison. Data shown belong to one representative mouse/group and are representative of two experiments with 2 or 3 mice/group each. **(B)** Column graphs showing the expression of Qa-1^b as geometric MFI (GMFI) in the indicated cell types from B6 mice that were naive or at 5 dpi with ECTV. Data are representative of two similar experiments with a total of 2 or 3 mice/group. Data were analyzed using ANOVA with correction for multiple comparisons. **(C)** Representative expression of Qa-1^b in B cells and MOs from the spleens of B6, *H2-T23$^{-/-}$*, and *H2-T23^{R72A}* mice that were naive or at 5 dpi with ECTV. Data correspond to a representative mouse per group and are representative of two experiments with 2 or 3 mice/group. **(D)** The indicated mice were infected with 3,000 pfu ECTV in the footpad, and survival was monitored. Data are displayed as a combination of four independent experiments with a total of 10–31 mice/group. Data were analyzed using the log-rank test. **(E)** B6 and *H2-T23^{R72A}* mice were infected with ECTV, and at 3 and 7 dpi the virus loads in spleens of individual mice were determined by plaque assay. Data are displayed as a combination of two independent experiments with a total of 10–19 mice/group. Data were analyzed using the *t* test. For all statistics in the figure, *, P ≤ 0.05; **, P ≤ 0.01; ***, P ≤ 0.001; ****, P ≤ 0.0001.

activating CD94–NKG2C/E, as we previously proposed, the role of Qa-1^b in resistance to mousepox could be in protecting uninfected bystander cells from detrimental killing by ECTV-activated NK cells through inhibitory CD94-NKG2A interaction.

NK cells activated by ECTV infection preferentially kill Qa-1^b–deficient uninfected targets in vitro and in vivo

To explore the possibility that Qa-1^b was important to protect bystander cells from ECTV-activated NK cell killing, NK cells purified from spleens of mice either naive or at 5 dpi with ECTV were added to monolayers of B6 or *H2-T23$^{-/-}$* BMDMs. After 4 h of coculture, BMDM viability was determined by real-time cell analysis (RTCA) using an xCELLigence instrument (Agilent; Fig. 5 A). The results demonstrated that NK cells obtained from ECTV-infected mice killed B6 and *H2-T23$^{-/-}$* BMDMs significantly better than NK cells obtained from naive mice. However, ECTV-activated NK cells were also significantly more efficient at

killing *H2-T23$^{-/-}$* than B6 BMDMs (Fig. 5 B). Therefore, NK cells activated by ECTV infection are poised to kill uninfected cells, such as primary BMDMs, and the killing is more efficient when the target cells do not express Qa-1^b.

To test whether the preferential killing of uninfected *H2-T23$^{-/-}$* cells by ECTV-activated NK cells also occurred in vivo, we mixed carboxyfluorescein succinimidyl ester (CFSE)–labeled WT (CD45.1) and *H2-T23$^{-/-}$* (CD45.2) splenocytes in a 1:1 ratio and adoptively transferred them into naive or ECTV-infected mice at 5 dpi. Mice were also depleted of NK cells to determine their possible role. At 18 h after transfer, the recipient mice were euthanized, and the CFSE-labeled cells in the spleens were identified by flow cytometry (Fig. 5 C). Results showed that in naive mice, whether depleted of NK cells or not, the ratios of transferred WT and *H2-T23$^{-/-}$* cells were similar to input ratios. On the other hand, in mice infected with ECTV, there was preferential disappearance of *H2-T23$^{-/-}$* cells, which
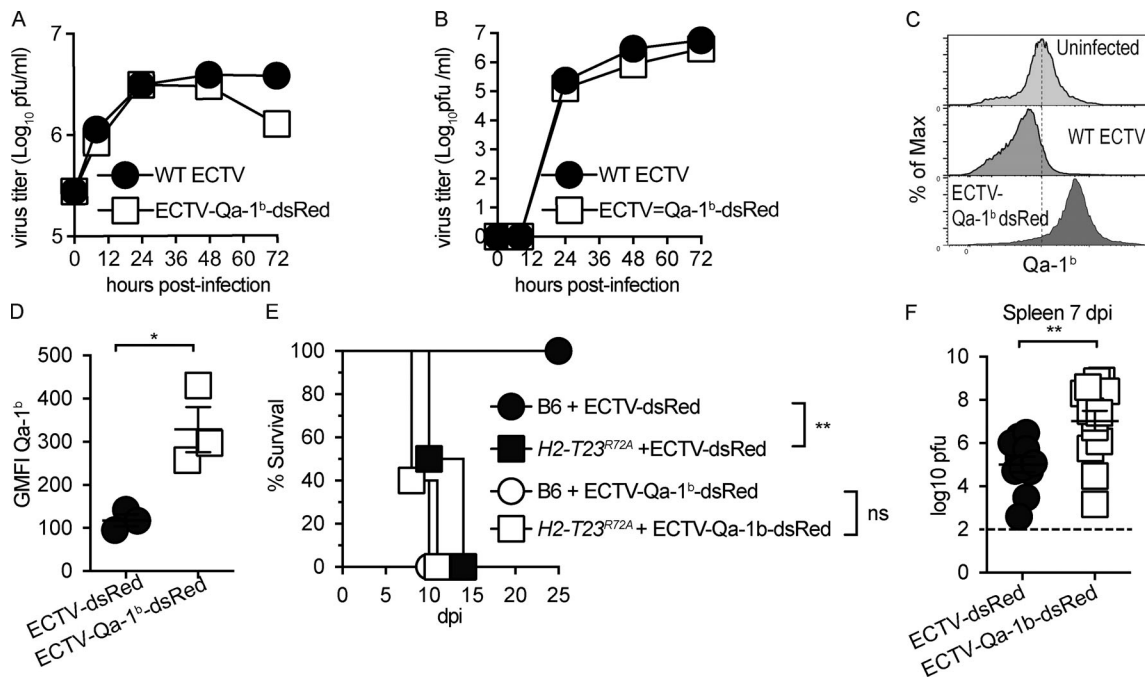
Figure 3. **Ectopic expression of Qa-1[b] in infected cells increases susceptibility to mousepox. (A)** Single-step growth of WT ECTV and ECTV–Qa-1[b] as determined by infecting monolayers of BS-C-1 cells with 5 pfu/cell for the indicated times and then determining virus titers in cell lysates. **(B)** Multistep growth of WT ECTV and ECTV–Qa-1[b] determined as in A except that the BS-C-1 cells were initially infected with 0.01 pfu/cell. **(C)** Qa-1[b] expression in BMDMs from B6 mice that were uninfected or infected overnight with 5 pfu/cell of WT-ECTV or ECTV–Qa-1[b]–dsRed. Data are representative of two similar experiments. The vertical dashed line intersects the MFI of the uninfected sample and is placed to facilitate the visual comparison of the histograms. **(D)** Qa-1[b] expression as GMFI in dsRed+ cells from the dLNs of B6 mice at 3 dpi with ECTV-dsRed or ECTV–Qa-1[b]–dsRed. Data are representative of two similar experiments with a total of 6 mice/group. Data were analyzed using the t test. **(E)** B6 and H2-T23[R72A] mice were infected with 3,000 pfu of ECTV-dsRed or ECTV–Qa-1[b]–dsRed, and survival was monitored. Data correspond to one experiment with 2–5 animals/group and are representative of two similar experiments. Data were analyzed using the log-rank test. **(F)** B6 mice were infected with ECTV-dsRed or ECTV–Qa-1[b]–dsRed, and at 7 dpi the virus loads in the spleens of individual mice were determined by plaque assay. Data correspond to two individual experiments combined with a total of 14–20 mice/group. Data were analyzed using the t test. For all statistics in the figure, *, $P \leq 0.05$; **, $P \leq 0.01$. GMFI, geometric MFI.

was significantly abrogated by NK cell depletion (Fig. 5 D). Therefore, NK cells activated by viral infection preferentially killed cells that do not express Qa-1[b] in vivo. Similar results were obtained in intact or NK cell–depleted mice that received a mixture of splenocytes from WT and H2-T23[R72A] mice (Fig. 1 E). Together, these data demonstrate that Qa-1[b] interaction with CD94-NKG2 on NK cells protects uninfected cells from killing by virus-activated NK cells.

Discussion

Previous work from other laboratories and ours has shown the important role that NK cells play in resistance to mousepox (Fang et al., 2008; Jacoby et al., 1989; Parker et al., 2007). We also showed that the NK cell–activating receptor NKG2D contributes to resistance to mousepox (Fang et al., 2008) and subsequently established an essential role for CD94 and its ligand Qa-1[b] in the early control of ECTV and mousepox survival (Fang et al., 2011). The up-regulation of Qa-1[b] in A9 cells (America Type Culture Collection [ATCC] CCL-1.4) infected with 1 pfu/cell ECTV in vitro (without differentiating infected from uninfected cells) and experiments with reporter assays suggested but did not prove that NK cells might recognize ECTV-infected cells via activating CD94-NKG2s in a Qa-1[b]–dependent manner (Fang et al., 2011).

Yet, a more thorough study was necessary to prove this hypothesis. In this manuscript, we delved deeper to understand how the interaction of CD94-NKG2 in NK cells and Qa-1[b] in target cells contributes to mousepox resistance.

First, we created Klrc3^{−/−} and Klrc2^{−/−} mice and found that they were mostly resistant to lethal mousepox. These results indicated that the absence of activating CD94-NKG2s cannot explain the extreme susceptibility of CD94-deficient mice. Yet, activating CD94-NKG2 heterodimers seem to play some role in the control of ECTV, as a few Klrc3^{−/−} mice succumbed to the infection and some had increased virus loads, while Klrc2^{−/−} mice had increased virus loads. Perhaps, we could get a better understanding with mice deficient in both NKG2C and NKG2E. Unfortunately, the two genes are tightly linked. Therefore, double-deficient mice cannot be generated by crossing and would require creating them de novo. However, it is possible that NKG2C/NKG2E double-deficient mice will not yield clarifying results because our data suggest that NK cells express NKG2C on the cell surface but not NKG2E. As we have shown, CD94 is expressed in most if not all NK cells compared with isotype control, and at least 50% stain with anti–NKG2C/E. Yet, in Klrc2^{−/−} mice, the staining with anti–NKG2C/E completely disappears and the CD94^{low} peak shifts almost to the level of the isotype control. On the other hand, in Klrc3^{−/−}
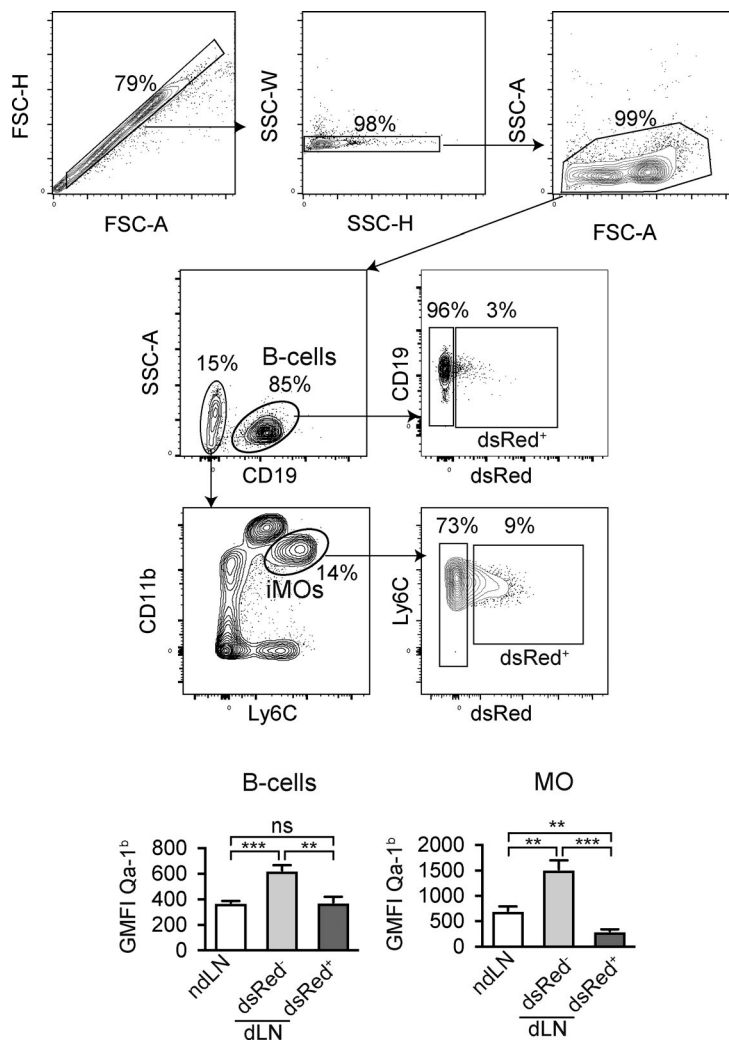
Figure 4. ECTV induces Qa-1^b down-regulation in infected and up-regulation in bystander MOs and B cells. Representative flow cytometry plots for the gating of infected (dsRed^+) and uninfected (dsRed^−) B cells (top) and iMOs (bottom) from the dLNs at 3 dpi with ECTV and graphs showing the expression of Qa-1^b in the indicated cells as mean ± SEM. Data are representative of two similar experiments with a total of 8–10 mice/group. Data were analyzed using ANOVA with correction for multiple comparisons. For all statistics in the figure, **, P ≤ 0.01; ***, P ≤ 0.001. GMFI, geometric MFI; ndLN, nondraining LN.

mice, staining with CD94, NKG2A, and anti–NKG2C/E remains similar to WT.

Next, we focused our attention on the CD94/NKG2 ligand, Qa-1^b. We confirmed previous results in our laboratory, showing that *H2-T23*^−/− mice are more susceptible to ECTV infection than WT B6 mice (Fang et al., 2011). Notably, we also found that *H2-T23*^R72A mice, which have a mutation in Qa-1^b that precludes interaction with CD94-NKG2 (Lu et al., 2007), were fully susceptible to lethal mousepox and had significantly higher virus loads than WT B6 mice. The reason why *H2-T23*^R72A mice are more susceptible to lethal mousepox than *H2-T23*^−/− mice will need further investigation. It is worthwhile to point out that *H2-T23*^R72A resemble *Klrd1*^−/−, which are also 100% susceptible. On the other hand, *Klrc1*^−/− (Rapaport et al., 2015) as well as *H2-T23*^−/− mice are partially susceptible to ECTV infection. *H2-T23*^−/− and *H2-T23*^R72A were originally made in a 129 background and backcrossed to B6 (Hu et al., 2004; Lu et al., 2007). Therefore, it is unlikely that genetic differences in the MHC between the two strains account for their difference in susceptibility. Whatever the reason, our data demonstrate that Qa-1^b is capable of interacting with CD94-NKG2 and is necessary for resistance to lethal mousepox.

Because lack of Qa-1^b confers susceptibility to mousepox, we attempted to rescue resistance in *H2-T23*^R72A mice by ectopically expressing WT Qa-1^b in ECTV. Contrary to our expectations, we found that rather than being attenuated in *H2-T23*^R72A mice, ECTV–Qa-1^b–dsRed was more pathogenic than ECTV WT in B6 mice. These results suggested that Qa-1^b expression prevented the killing of infected cells, which contradicted our previous hypothesis that Qa-1^b was elevated on infected cells, suggesting a protective role. To clarify this discrepancy, we took advantage of ECTV-dsRed to directly determine Qa-1^b expression in infected and noninfected iMOs and B cells in the dLNs of infected mice. The results demonstrated that only uninfected cells up-regulated Qa-1^b while infected iMOs down-regulated it, hinting that Qa-1^b expression may protect bystander cells from NK cell killing. To verify the protective role of Qa-1^b in uninfected cells, we used in vitro NK cell–mediated lysis and in vivo cell killing assay with or without NK cell depletion. In vitro, NK cells obtained from ECTV-infected mice lysed uninfected BMDMs if they were H2-T23^−/−. Consistently, uninfected splenocytes lacking Qa-1^b or bearing the R72A Qa-1^b mutation were also preferentially killed by NK cells in mice infected with ECTV but not in naive mice. These data indicate that bystander cells need to express Qa-1^b to avoid NK cell–mediated killing during viral infection. Of note, we previously demonstrated that uninfected iMOs play a major role in organizing a protective innate immune
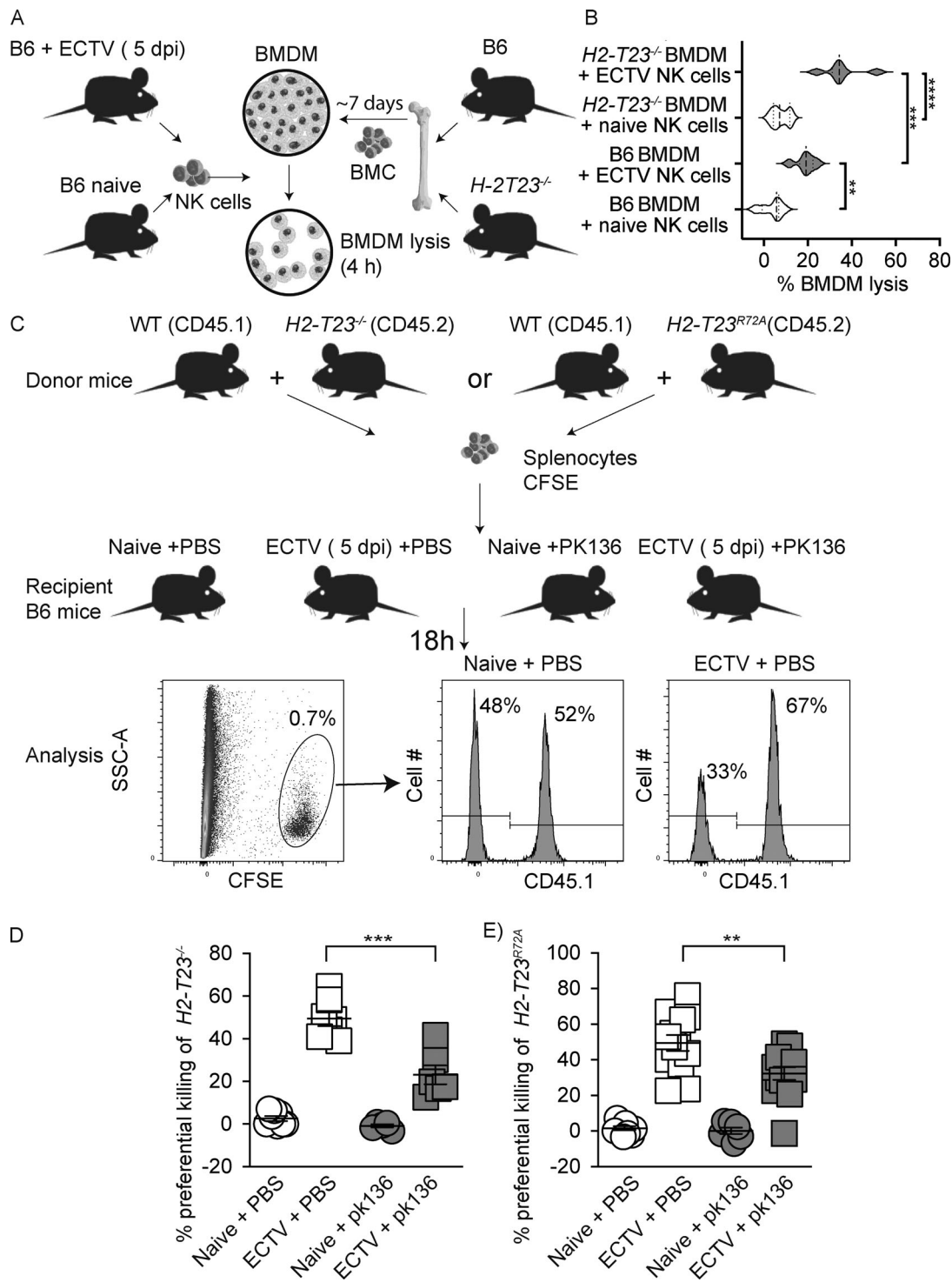
Figure 5. **NK cells activated by ECTV infection preferentially kill Qa-1^b–deficient uninfected targets in vivo. (A)** Graphical summary of the experimental procedure for in vitro killing of BMDMs: purified NK cells obtained from either naive or ECTV-infected mice at 5 dpi were added to monolayers of B6 or *H2-T23$^{-/-}$* BMDMs. After 4 h of co-culture, BMDM viability was determined by RTCA using an xCELLigence instrument (Agilent). **(B)** In vitro lysis of B6 BMDMs by the indicated NK cells. Data correspond to six individual experiments with duplicate wells. Data were analyzed using ANOVA with correction for multiple comparisons. **(C)** Graphical summary of in vivo killing experimental procedure. Single-cell suspensions of lymphocyte target cells from WT CD45.1$^+$ and *H2-T23$^{-/-}$* or *H2-T23^{R72A}* naive mice were mixed in a 1:1 ratio and labeled with 4 µM CFSE, and 2 × 10^7 total cells were injected intravenously into recipient naive or 5-d ECTV-infected B6 mice that had been depleted or not of NK cells with anti-NK1.1 mAb PK136 (200 µg) 24 h before cell transfer. After 18 h, the mice were killed, and the frequency of CFSE-labeled CD45.1$^+$ (WT) and CD45.1$^-$ (*H2-T23$^{-/-}$* or *H2-T23^{R72A}*) cells was determined by flow cytometry. The differential killing of Qa-1^b–deficient cells was determined as indicated in Materials and methods. **(D and E)** Preferential in vivo killing of H2-T23$^{-/-}$ (D) or H2-T23^{R72A} (E) cells in the indicated mice. The control mice were injected with PBS. Data are displayed as a combination of two or three independent experiments with a total of 5–14 mice/group. Data were analyzed using ANOVA with correction for multiple comparisons. For all statistics in the figure, **, $P \le 0.01$; ***, $P \le 0.001$; ****, $P \le 0.0001$.

response in the dLN that restricts early virus spread (Wong et al., 2018; Xu et al., 2015), and we have shown herein that ECTV spread is accelerated in $H2\text{-}T23^{R72A}$ mice. This suggests that the killing of uninfected iMOs in $H2\text{-}T23^{R72A}$ mice may play an important role in the susceptibility of this strain to ECTV. Future experiments will address this hypothesis.

In summary, our data indicate that the up-regulation of Qa-1^b in bystander cells functions as a "don't kill me" signal for NK cells, while its down-regulation in infected cells provides a "kill me" signal, a variation of the missing-self hypothesis (Bern et al., 2019; Kärre et al., 1986) where loss of Qa-1^b would relieve inhibitory signals. Yet, this switch function of Qa-1^b only occurs in NK cells activated by viral infection because resting NK cells do not preferentially kill $H2\text{-}T23^{-/-}$ or $H2\text{-}T23^{R72A}$ targets. These results provide a previously unknown mechanism for the regulation of NK cell antiviral function.

Materials and methods

Mice
All experiments were approved by the Thomas Jefferson University Institutional Animal Care and Use Committee. WT C57BL/6N mice (B6, B6-CD45.2) and B6.SJL-$Ptprc^aPepc^b$/BoyCrCrl (B6-CD45.1) mice were purchased from Charles River or bred in-house from breeders obtained from Charles River. CD94-deficient mice ($Klrd1^{-/-}$) backcrossed to a B6 background were previously described (Orr et al., 2010) and were bred at the Thomas Jefferson University Animal Facility. $H2\text{-}T23^{-/-}$ (Hu et al., 2004) and $H2\text{-}T23^{R72A}$ mice (Lu et al., 2007) in a B6 background were a kind gift from Dr. Harvey Cantor (Dana-Farber Cancer Institute, Boston, MA). All experiments were performed with a mixture of male and female mice except for those with $H2\text{-}T23^{-/-}$, where only males were used because this line displays extensive sexual dysmorphism in their response to ECTV, with most of the females being resistant.

$Klrc2^{-/-}$ mice were generated in our laboratory using the i-GONAD procedure of CRISPR/Cas9 gene editing performed as described by others (Gurumurthy et al., 2019; Ohtsuka et al., 2018) with a slight modification, which was the use of a Hamilton syringe instead of a mouth pipette to inject the CRISPR/Cas9 cocktail in the oviducts of B6 females (Charles River). This was followed by oviduct electroporation. The sequence of the CRISPR RNA, targeting exon 3, was 5′-AATCTTGGAATGACAGTTTG-3′, and the protospacer adjacent motif was GGG (Integrated DNA Technologies). The resulting $Klrc2^{-/-}$ mice have a GA insertion after position 438 of the transcript NM_010653.4), resulting in an early termination codon 40 bp downstream. For sequencing of the mutation, primers 5′-CTCTACCTGGTCACTTTCAGCTC-3′ and 5′-GCGTATGGGGAACATGGGAAT-3′ were used. Mutant mice were identified by flow cytometry or by PCR genotyping using the forward primers WT-specific F-WT-$Klrc2$ (5′-ATCTTGGAATGACAGTTTGGG-3′) or mutant-specific F-Mut-$Klrc2$ (5′-TCTTGGAATGACAGTGATTGG-3′) together with the reverse common primer R-Com-$Klrc2$ (5′-ATGCAGAGTGAAGAGACATGG-3′). Conditions for PCR were 94°C for 2 min, 35 cycles of 94°C for 30 s, 66°C for 30 s, 72°C for 30 s, and final extension at 72°C for 5 min.

To generate $Klrc3^{-/-}$ mice, B6 agouti (JM8A3.N1)–targeted Klrc3$^{tm1(KOMP)}$ ES cells were purchased from the Mutant Mouse Resource and Research Center at the University of California, Davis, a National Institutes of Health–funded strain repository. These ES cells were originally created by Pieter de Jong, Kent Lloyd, William Skarnes, and Allan Bradley at the Wellcome Sanger Institute and donated to the Mutant Mouse Resource and Research Center by The KOMP Repository at the University of California, Davis. Klrc3$^{tm1(KOMP)}$ ES cells had the $Klrc3$ gene (NCBI Reference Sequence NC_000072.7, *Mus musculus* strain C57BL/6J chromosome 6, GRCm39, accession no. NC_000072 REGION: complement [129613226..129620474]) with positions 1214–4792 comprising exons 3–5 and part of the flanking introns replaced by a 7,122-bp cassette containing the Neo and LacZ genes as well as LoxP and FRT sequences for Neo or Neo and LacZ removal by *Cre* or *Flippase* (Flp) recombinases, respectively. Klrc3$^{tm1(KOMP)}$ ES cells were injected into blastocysts, which were then transferred to surrogate mothers by the Fox Chase Cancer Center Tissue Culture and Transgenic Mouse facilities. Chimeric mice were identified by agouti coat color and bred to WT B6 mice. An F1 carrier was identified by a PCR amplicon of 722 bp when using tail DNA and forward neo specific primer (F-neo; 5′-GGGATCTCATGCTGGAGTTCTTCG-3′) corresponding to positions 6653–6676 of the cassette and the reverse primer R 5018-5045 of the WT $Klrc3$ gene. The progeny of the founder mouse was bred to homozygosity to produce mice deficient in $Klrc3$ with an inserted Neo/LacZ cassette ($Klrc3^{nl/nl}$). The definitive $Klc3^{-/-}$ strain was generated by crossing $Klrc3^{nl/nl}$ mice with B6;SJL-Tg(ACTFLPe)9205Dym (Stock No: 003800; The Jackson Laboratory) carrying *Flp* to remove most of the cassette. $Klrc3^{-/-}$ mice contained positions 1214–4792 (3,578 bp) of $Klrc3$ replaced by a 218-bp leftover from the cassette containing single FRT and LoxP sites. Homozygous $Klrc3^{-/-}$ mice were identified by the presence of a mutant-specific PCR amplicon of 592 bp when using tail DNA and primers F 1092–1119 of the $Klrc3$ gene and R 5018-5045, as well as absence of a WT PCR amplicon of 293 bp with primers F 4753-4779 and R 5018-5045. The identity of the 592-bp mutant band was verified by Sanger sequencing. $Klrc3^{-/-}$ mice lacking the Flp gene were selected for further breeding.

Viruses and infection
ECTV (strain Moscow) was obtained from ATCC (#VR-1374). ECTV-GFP and ECTV-dsRed were previously described (Fang et al., 2008; Roscoe et al., 2012). ECTV–Qa-1^b–dsRed was generated by standard homologous recombination using a virus deficient in EVM036 as previously described (Roscoe et al., 2012). All ECTV strains were propagated in tissue culture as previously described (Xu et al., 2008). Mice were infected in the left hind footpad with 3,000 pfu ECTV. For survival analysis, mice were monitored daily, being euthanized when they showed signs of imminent death (lack of movements and unresponsiveness to touch) and were recorded as dead. Euthanasia was performed according to the 2013 edition of the American Veterinary Medical Association Guideline for the Euthanasia of Animals. For virus titers, spleens or livers were homogenized in 2.5% FBS RPMI (Corning) using a TissueLyser (QIAGEN). Virus

Ferez et al.
Qa-1^b in viral infection

Journal of Experimental Medicine
https://doi.org/10.1084/jem.20201782

10 of 13

titers were determined on BS-C-1 cells as previously described (Xu et al., 2008).

Tissue culture

For ECTV growth and titration, we used BS-C-1 cells (#CCL-26; ATCC). Ba/F3 cells coexpressing CD94 and NKG2E (CT785) or CD94 and NKG2C (CT750) were a gift from Dr. Lewis L. Lanier (University of California, San Francisco, San Francisco, CA) and have been described previously (Fang et al., 2011). BMDMs were produced from bone marrow cells grown in supernatant of A9 cells (CCL-1.4; ATCC) as previously described (Ramirez and Sigal, 2002). For cell culture, we used RPMI-1640 tissue culture medium (Invitrogen Life Technologies) supplemented with 10% FCS (Sigma-Aldrich), 100 IU/ml penicillin and 100 μg/ml streptomycin (Invitrogen Life Technologies), 10 mM Hepes buffer (Invitrogen Life Technologies), and 0.05 mM 2-ME (Sigma-Aldrich). For virus growth and titers, RPMI with 2.5% FCS was used. All cells were grown at 37°C with 5% CO_2.

In vivo depletion of NK cells

Depletion of NK cells in B6 mice was performed by i.p. inoculation of 200 μg NK1.1 mAb PK136 24 h before adoptive cell transfer as before (Fang et al., 2008).

Flow cytometry

Flow cytometry was performed as described previously (Fang et al., 2008; Fang et al., 2011; Fang and Sigal, 2010; Xu et al., 2008). Briefly, LNs and spleens were obtained from mice and suspended in single-cell suspensions. Nonspecific binding of mAbs to the Fc receptor was blocked with antibody 2.4G2 (anti–Fc-g II/III receptor; ATCC), followed by surface and/or intracellular staining. We used the following antibodies: anti–Qa-1(b) (clone 6A8.6F10.1A6; biotin, BD Biosciences), Streptavidin (APC, PE-Cy7), anti-CD3ε (clone 145-2C11; FITC, Pacific Blue, PE-Cy7), anti-CD3 (clone 17A2; Brilliant Violet 785), anti-TCRβ (clone H57-597; PB, BV 785), anti-NKp46 (clone 29A1.4; APC, PE-Cy7), anti-NK1.1 (clone PK136; APC, BV 605, PE-Cy7), anti-CD45 (clone 30-F11; PerCP-Cy5.5), anti-CD27 (clone LG.3A10; PerCP-Cy5.5), anti-CD45.1 (clone A20; PB), anti-CD45.2 (clone 104; PE), anti-CD11b (clone M1/70; BV 605, PE-Cy7), anti-CD49b (clone DX5; APC), anti-CD94 (clone18d3; FITC, PE, eBioscience; BV 421, BD Biosciences), anti-Ly49H (clone 3D10; FITC, PE), anti–NKG2A/C/E (clone 20d5; FITC; eBioscience), anti-NKG2A[B6] (clone 16a11; PE, eBioscience), anti-NKG2D (clone CX5; APC), anti-NKG2C/E (clone 2098A; Unconjugated, R&D Systems), normal rabbit IgG (clone 60024B; Unconjugated, R&D Systems), anti-rabbit donkey IgG (Poly4064; Alexa Fluor647), anti-CD69 (clone H1.2F3; FITC), anti–Ly-6C (clone HK1.4; PerCP), anti-CD19 (clone 6D5; PerCP/Cy5.5), anti-CD127 (clone SB/199; APC), anti-B220 (clone RA3-6B2; PerCP/Cy5.5), anti–KLRG-1 (clone 2F1/KLRG1; PE-Cy7), anti–Ly49C/I (clone 5E6; FITC, BD Biosciences), anti-Ly49D (clone 4E5; PE), Ly49G2 (clone eBio4D11; FITC, eBioscience), anti-Ly49H (clone 3D10; PE), and anti-Eomes (clone Dan11mag; PE-Cy7, eBioscience). All antibodies and any corresponding isotype antibodies were purchased from Biolegend unless otherwise stated. For Eomes staining, extracellular molecules were stained as described

above, and cells were incubated in eBioscience intracellular fixation and permeabilization buffer (Thermo Fisher) for 40 min at 4°C. Cells were stained with anti-Eomes antibody in permeabilization buffer (Thermo Fisher). Cells were analyzed at the Thomas Jefferson University Flow Cytometry Facilities using LSR II and Fortessa instruments (Becton Dickinson).

In vitro cytotoxicity assay

In vitro NK cell killing of bone marrow macrophages was determined using an xCELLigence RTCA instrument (Agilent). For this purpose, 40,000 B6 or $H2\text{-}T23^{-/-}$ BMDMs (target cells) were seeded in individual wells of e-plates (Agilent), placed in the RTCA instrument chamber, and incubated at 37°C until the cell index (CI) as read by the instrument reached a plateau (~24 h). NK cells were isolated from naive and 5-dpi B6 splenocytes using the MojoSort Mouse NK Cell Isolation Kit (Biolegend) according to the manufacturer's instructions, and the purity was assessed by flow cytometry. Purified NK cells (effector cells) were added to each well of BMDMs in a 20:1 effector-target cell ratio. The CI observed at 4 h following effector cell addition was used to determine cell lysis according to the formula % lysis = CI no effector – CI effector/CI no effector × 100.

In vivo cytotoxicity assay

Whole splenocytes were isolated from B6-CD45.1 (CD45.1+ CD45.2−) and $H2\text{-}T23^{-/-}$ (CD45.1−CD45.2+) or $H2\text{-}T23^{R72A}$ (CD45.1−CD45.2+) mice mixed in a 1:1 ratio, stained with 4 μM CFSE, and 2 × 10⁷ cells were injected intravenously into recipient mice that had been infected or not with ECTV 5 d earlier. After 18 h, mice were euthanized, and spleens were processed into single-cell suspensions and analyzed by flow cytometry. Preferential killing was calculated based on the ratio of CD45.1+ and CD45.2+ frequencies of CFSE-labeled cells obtained before the injection. To calculate specific lysis after transfer, the following formula was used: % specific lysis = [1 – (ratio after transfer/ratio before transfer)] × 100, where "ratio" is % CD45.2/% CD45.1. Therefore, a positive specific lysis number indicates preferential killing of CD45.2+ cells, whereas a negative number implies preferential killing of CD45.1+ cells. A specific killing value of zero would suggest no preferential killing.

Statistical analysis

Data were analyzed with Prism 6 software (GraphPad). For survival, we used the log-rank (Mantel-Cox) test. For other experiments, ANOVA with Tukey correction for multiple comparisons or Student's t test was used as applicable. For all figures, *, $P < 0.05$, **, $P < 0.01$, ***, $P < 0.001$, ****, $P < 0.0001$.

Online supplemental material

Fig. S1 shows a diagram of the *Klrc3* gene with the 3,578-bp deletion/218-bp insertion in $Klrc3^{-/-}$ mice and the localization of the primers used for genotyping in Fig. 1 E; partial trace corresponding to the Sanger sequencing of the 592-bp amplicon resulting from the genotyping of Klrc3$^{-/-}$ mice; the phenotyping of WT, $H2\text{-}T23^{-/-}$, $H2\text{-}T23^{R72A}$, $Klrc3^{-/-}$, and $Klrc2^{-/-}$ NK cells as determined by flow cytometry using various mAbs; and partial traces corresponding to the Sanger sequencing of the 578-bp

Ferez et al.
Qa-1b in viral infection

Journal of Experimental Medicine   11 of 13
https://doi.org/10.1084/jem.20201782

amplicon resulting from the PCR amplification of exon 3 from WT and *Klrc2$^{-/-}$* mice using genotyping primers.

Acknowledgments

Author contributions: M. Ferez, C.J. Knudson, A. Lev, and L.J. Sigal conceived and designed experiments and analyzed results. M. Ferez and L.J. Sigal co-wrote the paper. C.J. Knudson helped with the writing. M. Ferez, C.J. Knudson, A. Lev, and L. Tang performed experiments. L.J. Sigal conceived the initial idea and supervised the study. E.B. Wong, P. Alves-Peixoto, and C. Stotesbury helped with some experiments.

Disclosures: The authors declare no competing interests exist.

References

Bern, M.D., B.A. Parikh, L. Yang, D.L. Beckman, J. Poursine-Laurent, and W.M. Yokoyama. 2019. Inducible down-regulation of MHC class I results in natural killer cell tolerance. *J. Exp. Med.* 216:99–116. https://doi.org/10.1084/jem.20181076

Braud, V.M., D.S. Allan, C.A. O'Callaghan, K. Söderström, A. D'Andrea, G.S. Ogg, S. Lazetic, N.T. Young, J.I. Bell, J.H. Phillips, et al. 1998. HLA-E binds to natural killer cell receptors CD94/NKG2A, B and C. *Nature.* 391: 795–799. https://doi.org/10.1038/35869

Brownstein, D.G., P.N. Bhatt, L. Gras, and R.O. Jacoby. 1991. Chromosomal locations and gonadal dependence of genes that mediate resistance to ectromelia (mousepox) virus-induced mortality. *J. Virol.* 65:1946–1951. https://doi.org/10.1128/JVI.65.4.1946-1951.1991

Call, M.E., K.W. Wucherpfennig, and J.J. Chou. 2010. The structural basis for intramembrane assembly of an activating immunoreceptor complex. *Nat. Immunol.* 11:1023–1029. https://doi.org/10.1038/ni.1943

Delano, M.L., and D.G. Brownstein. 1995. Innate resistance to lethal mousepox is genetically linked to the NK gene complex on chromosome 6 and correlates with early restriction of virus replication by cells with an NK phenotype. *J. Virol.* 69:5875–5877. https://doi.org/10.1128/JVI.69.9.5875-5877.1995

Diefenbach, A., and D.H. Raulet. 2001. Strategies for target cell recognition by natural killer cells. *Immunol. Rev.* 181:170–184. https://doi.org/10.1034/j.1600-065X.2001.1810114.x

Fang, M., and L. Sigal. 2010. Studying NK cell responses to ectromelia virus infections in mice. *Methods Mol. Biol.* 612:411–428. https://doi.org/10.1007/978-1-60761-362-6_28

Fang, M., L.L. Lanier, and L.J. Sigal. 2008. A role for NKG2D in NK cell-mediated resistance to poxvirus disease. *PLoS Pathog.* 4:e30. https://doi.org/10.1371/journal.ppat.0040030

Fang, M., F. Roscoe, and L.J. Sigal. 2010. Age-dependent susceptibility to a viral disease due to decreased natural killer cell numbers and trafficking. *J. Exp. Med.* 207:2369–2381. https://doi.org/10.1084/jem.20100282

Fang, M., M.T. Orr, P. Spee, T. Egebjerg, L.L. Lanier, and L.J. Sigal. 2011. CD94 is essential for NK cell-mediated resistance to a lethal viral disease. *Immunity.* 34:579–589. https://doi.org/10.1016/j.immuni.2011.02.015

Fehniger, T.A., S.F. Cai, X. Cao, A.J. Bredemeyer, R.M. Presti, A.R. French, and T.J. Ley. 2007. Acquisition of murine NK cell cytotoxicity requires the translation of a pre-existing pool of granzyme B and perforin mRNAs. *Immunity.* 26:798–811. https://doi.org/10.1016/j.immuni.2007.04.010

Gurumurthy, C.B., M. Sato, A. Nakamura, M. Inui, N. Kawano, M.A. Islam, S. Ogiwara, S. Takabayashi, M. Matsuyama, S. Nakagawa, et al. 2019. Creation of CRISPR-based germline-genome-engineered mice without ex vivo handling of zygotes by i-GONAD. *Nat. Protoc.* 14:2452–2482. https://doi.org/10.1038/s41596-019-0187-x

Hu, D., K. Ikizawa, L. Lu, M.E. Sanchirico, M.L. Shinohara, and H. Cantor. 2004. Analysis of regulatory CD8 T cells in Qa-1-deficient mice. *Nat. Immunol.* 5:516–523. https://doi.org/10.1038/ni1063

Jacoby, R.O., P.N. Bhatt, and D.G. Brownstein. 1989. Evidence that NK cells and interferon are required for genetic resistance to lethal infection with ectromelia virus. *Arch. Virol.* 108:49–58. https://doi.org/10.1007/BF01313742

Kabat, J., F. Borrego, A. Brooks, and J.E. Coligan. 2002. Role that each NKG2A immunoreceptor tyrosine-based inhibitory motif plays in mediating the human CD94/NKG2A inhibitory signal. *J. Immunol.* 169:1948–1958. https://doi.org/10.4049/jimmunol.169.4.1948

Kärre, K., H.G. Ljunggren, G. Piontek, and R. Kiessling. 1986. Selective rejection of H-2-deficient lymphoma variants suggests alternative immune defence strategy. *Nature.* 319:675–678. https://doi.org/10.1038/319675a0

Lanier, L.L. 1998. NK cell receptors. *Annu. Rev. Immunol.* 16:359–393. https://doi.org/10.1146/annurev.immunol.16.1.359

Le Dréan, E., F. Vély, L. Olcese, A. Cambiaggi, S. Guia, G. Krystal, N. Gervois, A. Moretta, F. Jotereau, and E. Vivier. 1998. Inhibition of antigen-induced T cell response and antibody-induced NK cell cytotoxicity by NKG2A: association of NKG2A with SHP-1 and SHP-2 protein-tyrosine phosphatases. *Eur. J. Immunol.* 28:264–276. https://doi.org/10.1002/(SICI)1521-4141(199801)28:01<264::AID-IMMU264>3.0.CO;2-O

Lee, N., M. Llano, M. Carretero, A. Ishitani, F. Navarro, M. López-Botet, and D.E. Geraghty. 1998. HLA-E is a major ligand for the natural killer inhibitory receptor CD94/NKG2A. *Proc. Natl. Acad. Sci. USA.* 95: 5199–5204. https://doi.org/10.1073/pnas.95.9.5199

Long, E.O. 1999. Regulation of immune responses through inhibitory receptors. *Annu. Rev. Immunol.* 17:875–904. https://doi.org/10.1146/annurev.immunol.17.1.875

Lu, L., K. Ikizawa, D. Hu, M.B. Werneck, K.W. Wucherpfennig, and H. Cantor. 2007. Regulation of activated CD4+ T cells by NK cells via the Qa-1-NKG2A inhibitory pathway. *Immunity.* 26:593–604. https://doi.org/10.1016/j.immuni.2007.03.017

Ohtsuka, M., M. Sato, H. Miura, S. Takabayashi, M. Matsuyama, T. Koyano, N. Arifin, S. Nakamura, K. Wada, and C.B. Gurumurthy. 2018. i-GONAD: a robust method for in situ germline genome engineering using CRISPR nucleases. *Genome Biol.* 19:25. https://doi.org/10.1186/s13059-018-1400-x

Orr, M.T., J. Wu, M. Fang, L.J. Sigal, P. Spee, T. Egebjerg, E. Dissen, S. Fossum, J.H. Phillips, and L.L. Lanier. 2010. Development and function of CD94-deficient natural killer cells. *PLoS One.* 5:e15184. https://doi.org/10.1371/journal.pone.0015184

Parker, A.K., S. Parker, W.M. Yokoyama, J.A. Corbett, and R.M. Buller. 2007. Induction of natural killer cell responses by ectromelia virus controls infection. *J. Virol.* 81:4070–4079. https://doi.org/10.1128/JVI.02061-06

Ramirez, M.C., and L.J. Sigal. 2002. Macrophages and dendritic cells use the cytosolic pathway to rapidly cross-present antigen from live, vaccinia-infected cells. *J. Immunol.* 169:6733–6742. https://doi.org/10.4049/jimmunol.169.12.6733

Rapaport, A.S., J. Schriewer, S. Gilfillan, E. Hembrador, R. Crump, B.F. Plougastel, Y. Wang, G. Le Friec, J. Gao, M. Cella, et al. 2015. The Inhibitory Receptor NKG2A Sustains Virus-Specific CD8+ T Cells in Response to a Lethal Poxvirus Infection. *Immunity.* 43:1112–1124. https://doi.org/10.1016/j.immuni.2015.11.005

Roscoe, F., R.H. Xu, and L.J. Sigal. 2012. Characterization of ectromelia virus deficient in EVM036, the homolog of vaccinia virus F13L, and its application for rapid generation of recombinant viruses. *J. Virol.* 86: 13501–13507. https://doi.org/10.1128/JVI.01732-12

Saether, P.C., S.E. Hoelsbrekken, S. Fossum, and E. Dissen. 2011. Rat and mouse CD94 associate directly with the activating transmembrane adaptor proteins DAP12 and DAP10 and activate NK cell cytotoxicity. *J. Immunol.* 187:6365–6373. https://doi.org/10.4049/jimmunol.1102345

Sigal, L.J. 2016. The Pathogenesis and Immunobiology of Mousepox. *Adv. Immunol.* 129:251–276. https://doi.org/10.1016/bs.ai.2015.10.001

Sullivan, L.C., C.S. Clements, T. Beddoe, D. Johnson, H.L. Hoare, J. Lin, T. Huyton, E.J. Hopkins, H.H. Reid, M.C. Wilce, et al. 2007. The hetero-dimeric assembly of the CD94-NKG2 receptor family and implications for human leukocyte antigen-E recognition. *Immunity.* 27:900–911. https://doi.org/10.1016/j.immuni.2007.10.013

Sun, J.C., and L.L. Lanier. 2011. NK cell development, homeostasis and function: parallels with CD8+ T cells. *Nat. Rev. Immunol.* 11:645–657. https://doi.org/10.1038/nri3044

Vance, R.E., D.M. Tanamachi, T. Hanke, and D.H. Raulet. 1997. Cloning of a mouse homolog of CD94 extends the family of C-type lectins on murine natural killer cells. *Eur. J. Immunol.* 27:3236–3241. https://doi.org/10.1002/eji.1830271222

Vance, R.E., J.R. Kraft, J.D. Altman, P.E. Jensen, and D.H. Raulet. 1998. Mouse CD94/NKG2A is a natural killer cell receptor for the nonclassical major histocompatibility complex (MHC) class I molecule Qa-1(b). *J. Exp. Med.* 188:1841–1848. https://doi.org/10.1084/jem.188.10.1841

Vance, R.E., A.M. Jamieson, and D.H. Raulet. 1999. Recognition of the class Ib molecule Qa-1(b) by putative activating receptors CD94/NKG2C and CD94/NKG2E on mouse natural killer cells. *J. Exp. Med.* 190:1801–1812. https://doi.org/10.1084/jem.190.12.1801

Vance, R.E., A.M. Jamieson, D. Cado, and D.H. Raulet. 2002. Implications of CD94 deficiency and monoallelic NKG2A expression for natural killer cell development and repertoire formation. *Proc. Natl. Acad. Sci. USA.* 99: 868–873. https://doi.org/10.1073/pnas.022500599

Wallace, G.D., and R.M. Buller. 1985. Kinetics of ectromelia virus (mousepox) transmission and clinical response in C57BL/6j, BALB/cByj and AKR/J inbred mice. *Lab. Anim. Sci.* 35:41–46.

Wong, E., R.H. Xu, D. Rubio, A. Lev, C. Stotesbury, M. Fang, and L.J. Sigal. 2018. Migratory Dendritic Cells, Group 1 Innate Lymphoid Cells, and Inflammatory Monocytes Collaborate to Recruit NK Cells to the Virus-Infected Lymph Node. *Cell Rep.* 24:142–154. https://doi.org/10.1016/j.celrep.2018.06.004

Xu, R.H., M. Cohen, Y. Tang, E. Lazear, J.C. Whitbeck, R.J. Eisenberg, G.H. Cohen, and L.J. Sigal. 2008. The orthopoxvirus type I IFN binding protein is essential for virulence and an effective target for vaccination. *J. Exp. Med.* 205:981–992. https://doi.org/10.1084/jem.20071854

Xu, R.H., E.B. Wong, D. Rubio, F. Roscoe, X. Ma, S. Nair, S. Remakus, R. Schwendener, S. John, M. Shlomchik, and L.J. Sigal. 2015. Sequential Activation of Two Pathogen-Sensing Pathways Required for Type I Interferon Expression and Resistance to an Acute DNA Virus Infection. *Immunity.* 43:1148–1159. https://doi.org/10.1016/j.immuni.2015.11.015

Yokoyama, W.M., and W.E. Seaman. 1993. The Ly-49 and NKR-P1 gene families encoding lectin-like receptors on natural killer cells: the NK gene complex. *Annu. Rev. Immunol.* 11:613–635. https://doi.org/10.1146/annurev.iy.11.040193.003145

Zeng, L., L.C. Sullivan, J.P. Vivian, N.G. Walpole, C.M. Harpur, J. Rossjohn, C.S. Clements, and A.G. Brooks. 2012. A structural basis for antigen presentation by the MHC class Ib molecule, Qa-1b. *J. Immunol.* 188: 302–310. https://doi.org/10.4049/jimmunol.1102379
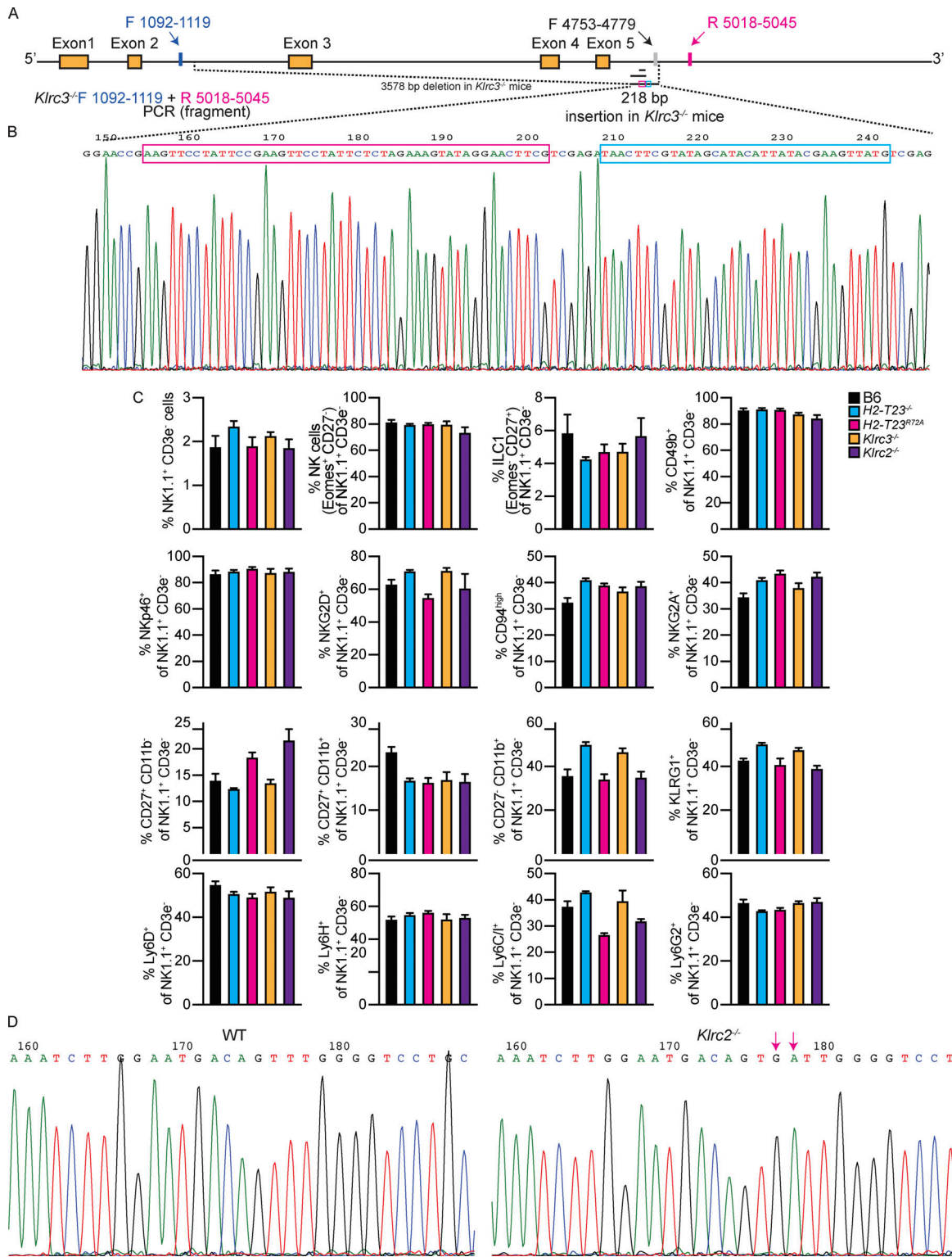
Supplemental material

Figure S1. **Characterization of mouse lines. (A)** Diagram of the *Klrc3* gene showing the 3,578-bp deletion/218-bp insertion in *Klrc3*^{−/−} mice and the localization of the primers used for genotyping in Fig. 1 E. **(B)** Partial trace corresponding to the Sanger sequencing of the 592-bp amplicon resulting from the PCR amplification using the indicated primers with DNA from *Klrc3*^{−/−} mice. The sequences of the residual FRT and LoxP sites are respectively boxed in magenta and cyan. **(C)** Flow cytometry analysis of splenocytes from the indicated mice with mAbs directed to the indicated markers. Data correspond to one representative experiment from two experiments with 3–5 mice/group in each (the experiment with R72A was performed only once with five mice due to lack of mice). Data were analyzed using ANOVA with correction for multiple comparisons. All comparisons were not significant. Error bars indicate mean ± SEM. **(D)** Partial traces corresponding to the Sanger sequencing of the 578-bp amplicon resulting from the PCR amplification of exon 3 from WT and *Klrc2*^{−/−} mice using primers 5′-CTC TACCTGGTCACTTTCAGCTC-3′ and 5′-GCGTATGGGGAACATGGGAAT-3′. The G and A insertions in the *Klrc2*^{−/−} gene are marked with magenta arrows.